Express Polymer Letters Vol.16, No.6 (2022) 607–623
Available online at www.expresspolymlett.com
https://doi.org/10.3144/expresspolymlett.2022.45

express polymer letters

Research article

Multifunctional gluten/guar gum copolymer with self-adhesion, self-healing, and remolding properties as smart strain sensor and self-powered device

Artjima Ounkaew[1], *Pornnapa Kasemsiri*[1*], *Natnaree Srichiangsa*[1], *Kaewta Jetsrisuparb*[1], *Jesper T. N. Knijnenburg*[2], *Manunya Okhawilai*[3], *Salim Hiziroglu*[4], *Somnuk Theerakulpisut*[5]

[1]Department of Chemical Engineering, Faculty of Engineering, Khon Kaen University, 40002 Khon Kaen, Thailand
[2]Biodiversity and Environmental Management Division, International College, Khon Kaen University, 40002 Khon Kaen, Thailand
[3]Metallurgy and Materials Science Research Institute, Chulalongkorn University, 10330 Bangkok, Thailand
[4]Department of Natural Resource Ecology and Management, Oklahoma State University, 303-G Agricultural Hall, Stillwater, OK 74078, USA
[5]Energy Management and Conservation Office, Faculty of Engineering, Khon Kaen University, 40002 Khon Kaen, Thailand

Received 1 December 2021; accepted in revised form 14 February 2022

Abstract. In this research, a multifunctional strain sensor based on gluten/guar gum (GG) copolymer was developed. The effects of gluten/GG blended ratios on the mechanical and electrical properties, self-adhesion, self-healing, remolding, self-powered and long-term stability of the strain sensors were studied. Among tested substrates, the gluten/GG blend indicated a strong adhesion to wood and paper substrates and showed a maximum adhesive strength at 1.5 wt% of GG in the copolymer (gluten/GG-1.5%). The adhesive strength of gluten/GG-1.5% decreased in the acceptable range when it was applied in 10 repeated adhesion cycles. The gluten/GG-1.5% exhibited a high electrical conductivity of 0.12 S/m and stretchability of 465%. The gluten/GG-based sensor containing glycerol showed long-term stability of self-healing, remolding, and self-powered ability when stored for 7 days, whereas the self-adhesive ability decreased with increasing storage time. The self-adhesive gluten/GG-1.5% was used to monitor human limb movements, which showed remarkable sensitivity during the storage time of 3 days. Such properties suggested a potential use of smart strain sensors with multifunctional capabilities for applications in wearable electronic devices.

Keywords: *smart polymers, strain sensor, biopolymers, self-adhesion, self-healing*

1. Introduction

Wearable and stretchable strain sensors have attracted much attention for monitoring human health situations [1–3]. The operational mechanism of strain sensors is based on the sensitivity of their resistance or capacitance to strain. Strain sensors with a high mechanical stretchability can be applied to monitor muscle or joint movements. Nowadays, most strain sensors are non-adhesive materials that are mounted on the skin using non-stretchable adhesive tape or bandage [4]. Such sensors present limitations in actual applications because the incomplete contact between the skin and the strain sensor may result in errors in detecting the body movement. Hence, an improvement in the contact between the skin and the strain sensors is often desirable. Consequently, researchers have focused on the development of self-adhesive strain sensors [5–7], such as the synthesis

*Corresponding author, e-mail: pornkas@kku.ac.th
© BME-PT

of mussel-inspired hydrogel [8] and fabrication of bi-layer strain sensor containing an adhesive layer [9]. Han *et al*. [10] suggested a method for the simple and environmentally friendly preparation of adhesive gluten-ionic skin sensors. The gluten-containing potassium chloride and glycerol could sense human movements. The obtained sensor could to several substrates, *viz*. hog skin, plastic, glass, paper, and stainless steel with an adhesive strength of 16.8–34.4 kPa.

Nowadays, not only the stability for movement sensing but also the smart properties of strain sensors are focused on [11, 12]. Such smart strain sensors are designed to have self-healing ability and long-term stability. Hydrogels containing borax and glycerol with long-term stability have been reported as self-healing strain sensors [13]. Glycerol is a cryoprotectant agent that can resist the freezing and drying of hydrogels suitable for long-term application [14]. When borax is incorporated into a hydrogel containing glycerol, the dynamic crosslinked network of glycerol-water-borax can be formed, which creates the self-healing ability [15].

Guar gum (GG) is a biopolymer that is generally derived from wheat flour in a food-producing process, in which the insoluble GG is separated from wheat flour. The main components of GG, such as glutenin and gliadin, are sticky and flexible [16]. These characteristics allow GG to be used as an adhesive. Pan *et al*. [17] studied the GG strain sensor containing borax and glycerol using GG extracted from guar seeds. The GG containing 4 wt% borax showed a complete gel form. The mended GG had a storage modulus comparable to the original sample.

Recently, the properties of strain sensors based on biopolymers have been developed by creating double networks that consist of more than one type of biopolymer [18, 19]. It was found that the mechanical properties and microstructures could be tuned by controlling the biopolymer composition [20, 21]. Li *et al*. [22] observed that double network hydrogels based on polyvinyl alcohol/polyethylene glycol had 6 times higher mechanical strength than the single network (polyvinyl alcohol). Rao *et al*. [23] fabricated a double network strain sensor using GG/alginate. The tensile strength of the strain sensors could be tuned by adjusting the GG/alginate ratio, and the highest tensile strength and self-healing efficiency were found with a GG/alginate ratio of 3/5. Hence, the fabrication of strain sensors with a double network would be an alternative approach to fine-tune the desired properties.

Smart strain sensors with unique properties can have versatile applications. However, most strain sensors need an external power source to properly drive their functions. Therefore, integrating a self-powered ability into strain sensors would add a valuable extra feature to the sensors, making them suitable for application in wearable electronic devices [24, 26]. Interestingly, strain sensors with ionic conductivity can be used as an ideal solid electrolyte for soft batteries. Some solid electrolytes such as gelatin crosslinked with tannic acid [25], catechol-chitosan hydrogel [27], and polyacrylic acid/nanochitin composite hydrogel [28] have been developed and applied as self-powered strain sensors. Although a number of studies have focused on fabricating self-powered strain sensors [29, 30], there is very little information on self-powered strain sensors with integrated smart functions such as self-adhesion, self-healing, and long-term stability.

This study aimed to develop a new smart strain sensor with integrated multifunctional properties *viz*. self-adhesion, self-healing, remolding, and the self-powered ability for long-term stability. The composition of the prepared smart strain sensor was based on blends of gluten and GG. Borax was used to create a dynamic crosslinked network, whereas glycerol was applied as cyoprotectant to achieve high long-term stability. The effects of the gluten/GG ratio on the sensor properties (*i.e*., mechanical properties, electrical conductivity, self-adhesion, self-healing, remolding, and self-powered ability) were investigated. Finally, the smart sensor was used to detect human limb movements.

2. Experimental

2.1 Materials

Wheat gluten and GG were purchased from a local supermarket in Khon Kaen, Thailand. Sodium tetraborate or borax (purity of 99.5%) and glycerol (purity of 99.5%) were obtained from Elago Enterprises Pty. Ltd. Glyceryl monostearate (GMS) was from Krungthepchemi Co., Ltd.

2.2. Preparation of gluten/GG smart strain sensor

The preparation process of the gluten/GG smart strain sensor is illustrated in Figure 1. The gluten solution was prepared by adding gluten (10 g) into a solution

consisting of glycerol (10 ml) and deionized water (30 ml) followed by stirring for 5 min. The GG solution was prepared separately by dissolving GG and GMS (12 mg) into a solution consisting of glycerol (2 ml) and deionized water (4 ml) at 95 °C for 20 min. The gluten solution was mixed with the obtained GG solution at 95 °C for 5 min. Next, borax solution (10 ml, 6.25 wt%/v) was added into the mixed gluten/GG solution and stirred for another 15 min at 95 °C. The gluten-containing 0, 0.5, 1.5, 3 and 5 wt% of GG were defined as gluten/ GG-0%, gluten/GG-0.5%, gluten/GG-1.5%, gluten/ GG-3% and gluten/GG-5%, respectively.

2.3. Characterization of gluten/GG smart strain sensor

The smart strain sensor samples were studied using attenuated total reflection Fourier transform infrared (ATR-FTIR) spectroscopy (Jasco 4200) at wavenumbers ranging from 4000 to 550 cm^{-1} with a resolution of 4 cm^{-1}.

To measure the adhesive strength, lap shear adhesion testing was performed according to the method previously described by Wang *et al*. [5] with minor modification. Here, 0.5 g of sample was placed onto three different substrates *viz*. glass, paper, and wood with a lap joint of 20 mm × 25 mm. A 500 g weight was pressed on the lap joint area to make the sample and substrate stick more tightly. The lap shear was tested using a Shimadzu SCG connected with a load cell of 5 kN at a pulling rate of 10 mm/min. The average values from five samples were determined. The stretchability of the strain sensor was achieved from the maximum strain limit [31]. The maximum strain of the sample was tested following the ASTM D 882-10 method.

Three-dimensional (3D) images, roughness, and size of the microgroove structure of the samples were analyzed using a confocal laser scanning microscope (CLSM, Olympus LEXT OLS5100).

The conductivity values of samples were calculated by Equation (1). The electrical resistance of the samples was measured using a two probe KEITHLEY model 2400. A voltage in the range of 0–12 V was applied for measurement. A Fluke 289 True RMS multimeter was used to detect simultaneous resistance changes under stimulus during joint bending:

$$\sigma = \frac{1}{R}\frac{L}{S} \tag{1}$$

where σ was the conductivity value [S/cm], L was the thickness [cm], S was the area [cm^2] and R was the resistance of the gluten/GG sample [Ω].

The freezing points of the samples were studied using a Netzsch DSC 214 Polyma differential scanning calorimeter (DSC). A sample of 3–5 mg was cooled from 20 to -20 °C with a cooling rate of 5 °C·min^{-1} under 40 ml·min^{-1} N_2 flow as the purge gas.

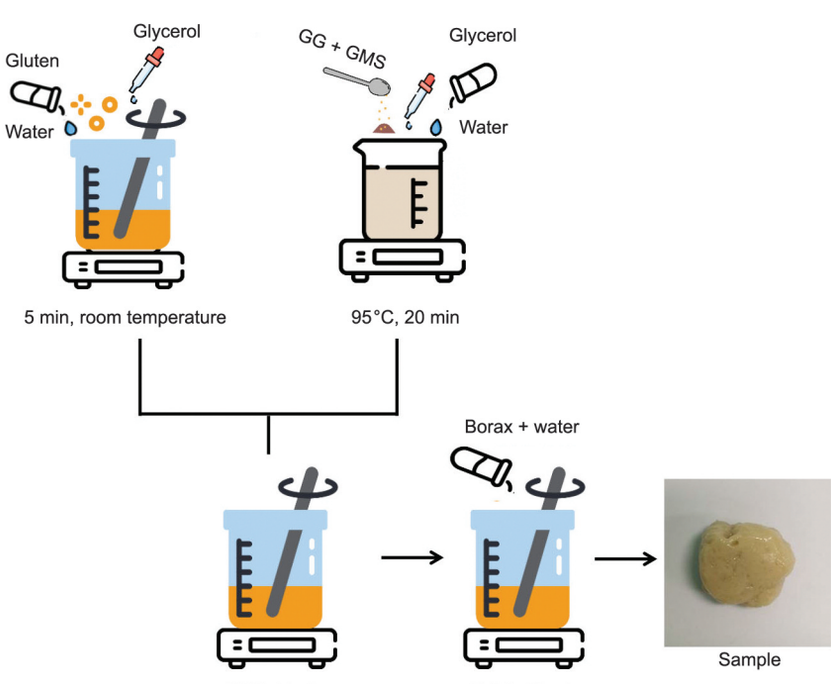

Figure 1. Schematic diagram of the preparation process of gluten/GG smart strain sensor.

The long-term stability of the samples was tested by examining the ionic conductivity, water retention capacity, self-healing, remolding, self-adhesion, and self-powered ability after storing the sample at 25 °C for 3, 5, and 7 days. The water retention capacity was calculated using Equation (2):

$$\text{Water retention capacity [\%]} = \frac{W_t}{W_0} \cdot 100 \qquad (2)$$

where W_t and W_0 are instantaneous and original weights of the sample, respectively.

3. Results and discussion

3.1. ATR-FTIR spectra of gluten/GG smart strain sensor

The ATR-FTIR spectra of gluten powder, GG powder, GMS, glycerol, and borax are presented in Figure 2a. The neat gluten showed strong amide peaks at 1637 and 1520 cm^{-1} that corresponded to C=O and N–H vibrations, respectively. The region of 3100–3500 cm^{-1} was assigned to N–H vibrations, which are typical for proteins. The GG powder showed broad absorption bands at 3319 and 1647 cm^{-1} attributed to O–H stretching and bending vibrations [17, 32], respectively. The peak at 2920 cm^{-1} was assigned to C–H stretching vibrations, whereas peaks at 1405 and 1150 cm^{-1} corresponded to C–H and C–O–C stretching vibrations, respectively. Glycerol had its main absorbance peak at 1034 cm^{-1} attributed to C–O stretching vibrations. The O–H peaks were located at 3290 cm^{-1} and 1413–1326 cm^{-1}, while C–H peaks were found at 2930 and 2880 cm^{-1} [33]. For borax, the major characteristic peaks were found at 3000–3500 cm^{-1}, which could be assigned to O–H vibrations, whereas the B–O stretching vibrations were observed at 1300–1600 and 813 cm^{-1} [34, 35]. The GMS showed characteristic peaks at 713 cm^{-1} for C–H bending vibrations, 1044 and 1170 cm^{-1} for C–O stretching vibrations, and 1725 cm^{-1} for C=O vibrations. The peak of O–H was observed at 3310 cm^{-1} [36]. The gluten/GG-1.5% hydrogel without borax showed only the main characteristic peaks of neat gluten and GG, as shown in Figure 2b. The gluten/GG-1.5% with borax showed the asymmetric stretching vibration of B–O linkages at 813 cm^{-1}. The peaks shift of O–H stretching vibrations (from 3290 to 3280 cm^{-1}) and C=O stretching vibrations (from 1652 to 1642 cm^{-1}) were observed when compared to gluten/GG without borax. This phenomenon indicated an interaction between the polymer matrix and borax through hydrogen bonding [17, 37–38].

3.2. Self-adhesion of gluten/GG strain sensor

Adhesion tests were performed to measure the adhesion of gluten/GG to common substrates, *viz*. wood, paper, and glass, which have been applied in wearable electronic applications [39–43]. Figure 3a shows a schematic illustration of the adhesion test. As can be seen in Figure 3b, all gluten/GG samples showed a similar trend in adhesive strength for three substrates with the following order: wood > paper > glass. Different surface

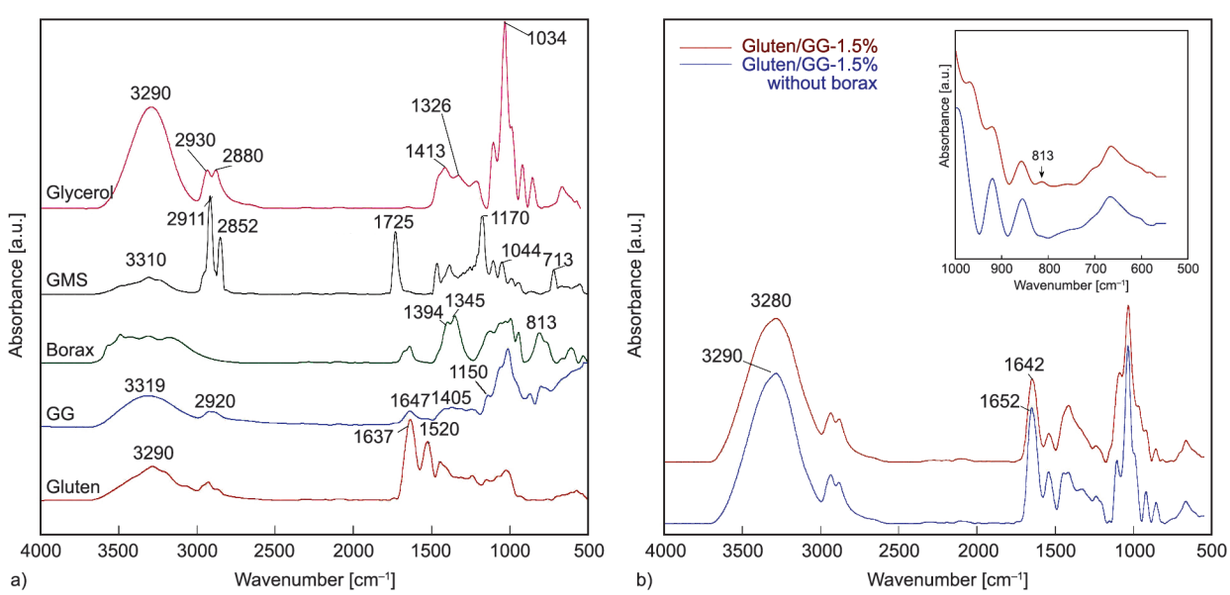

Figure 2. ATR-FTIR spectra of smart strain sensor (a) raw materials of smart strain sensor (b) gluten/GG-1.5% with and without borax.

energy and surface roughness that are responsible for the cohesion and adhesion of an adhesive [44]. For wood and paper, the greater adhesive strength is related to the polar groups and roughness on the surface when compared to glass. This result was in good agreement with the adhesion properties of pyrogallol-borax hydrogel with the highest adhesive strength for a wood substrate [45]. The high surface roughness of a substrate implies a high contact area between the substrate and hydrogel, resulting in good adhesive strength [32]. Figure 4 depicts the profilometry images, surface profiles and morphology of hydrogels with various gluten/GG ratios. Figures 4a and 4b show the color from 3D profiles and surface roughness profiles, respectively. The variation in color and roughness profile was clearly visible for gluten/GG-1.5% and gluten/GG-3% when compared to other samples. However, the morphology of gluten/GG-1.5% in Figure 4c showed a rougher surface than gluten/GG-3%. A suitable ratio of gluten/GG of the polymer blend provided the interaction between molecules such as hydrogen bonding, creating roughness and decreasing aggregation of the molecules. A high surface roughness of an adhesive could increase the contact area with substrates and enhance the interfacial adhesion [46, 47]. This observation corresponded to the highest adhesive strength of gluten/GG-1.5% for all three substrates (wood, paper and glass) as shown in Figure 3b. However, an improper ratio of the polymer blend might result in excess intermolecular interactions hence a smoother surface [48]. In addition, the adhesion ability of the polymer blend also depends on the balance between cohesion and adhesion. Wang *et al*. [49] observed that the addition of 2 wt% chitosan in polyacrylic hydrogel can improve the adhesive strength, while the adhesive strength decreased at higher chitosan contents. The excess chitosan hindered network formation that resulted in an increase of cohesion and decrease of adhesion. As shown in Figure 3b, the adhesive strength of gluten/GG ranged from 0.23±0.02 to 9.17±0.97 kPa. The obtained adhesion could be tailored by adjusting GG content. Furthermore, the adhesive strength values were in the same range as previous reports *viz*. wheat gluten strain sensor (0.013–0.07 kPa) [32], chitosan-polyoxometalate strain sensor (4.35±0.31–5.84±0.39 kPa) [50] and poly(vinylalcohol)/poly(acrylamide-*co*-[2-(methacryloyloxy) ethyl] dimethyl-(3-sulfo-propyl) ammonium hydroxide) hydrogel sensors (8.8–11.7 kPa) [30].

The gluten/GG-1.5% sample demonstrated the highest adhesive strength and was further tested for adhesion to various substrates such as hog skin, plastic, metal, pen, stainless steel, glass slide, wood, and paper, as shown in Figure 5a. The gluten/GG-1.5% had excellent adhesion to all substrates with different characteristics *viz*. hydrophilic, hydrophobic, and metallic. Glutenin, gliadin, and some amino acids in gluten are compatible with different surface features because of the van der Waals forces, hydrogen bonding, π–π stacking, electrostatic and hydrophobic interactions. The presence of hydroxyl groups of GG

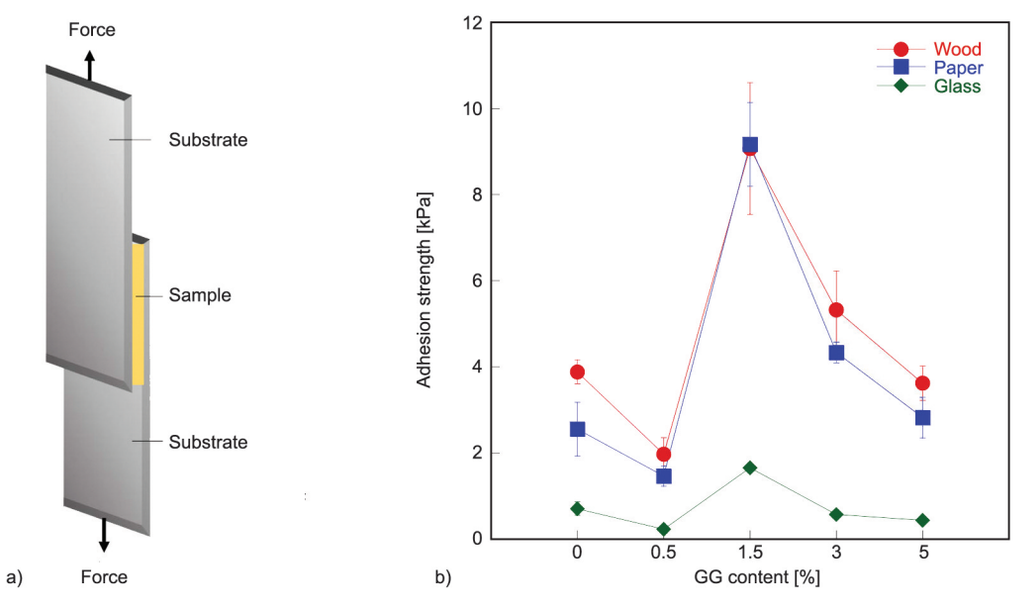

Figure 3. Adhesion of gluten/GG smart strain sensor: (a) schematic illustration of the lap shear test geometry and (b) adhesion strength of gluten/GG-1.5% for three substrates.

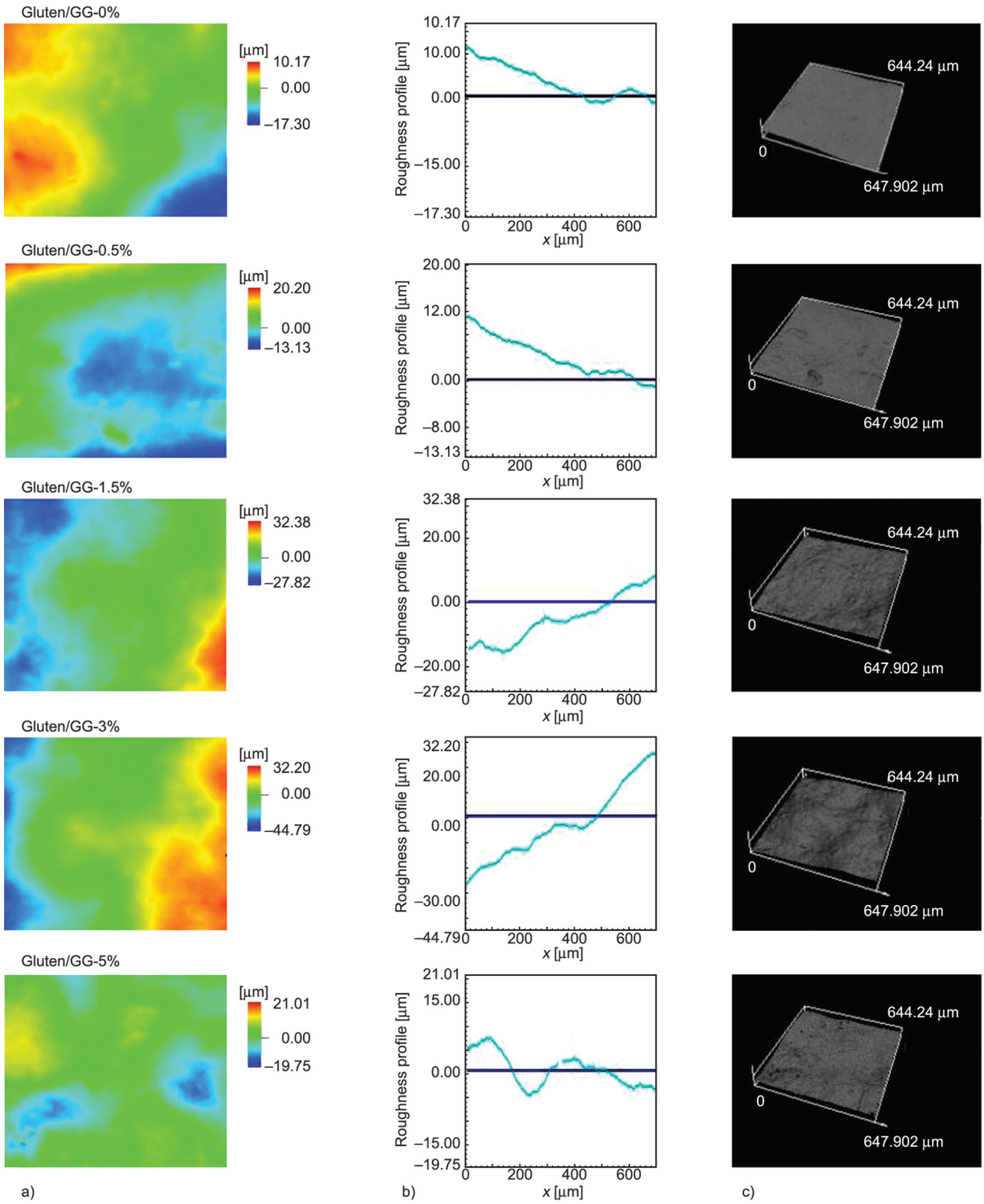

Figure 4. (a) profilometry images, (b) surface profiles, and (c) morphology of gluten/GG at various contents.

can participate in hydrogen bonding to create adhesion to hydrophilic substrates [32]. Chen *et al*. [51] observed that the blended GG with isolated soy protein adhesive increased hydrogen bonding, which led to an increase in adhesive bond strength. Furthermore, Figure 5b demonstrates that gluten/GG-1.5% could adhere to a hand, and no residue was observed when it was peeled off. Usually, the residue on the skin after use presents a concern because the self-adhesive sensor might stick to the skin and is hard to remove [5]. Furthermore, no obvious redness, skin injuries, and allergic reaction were found during the application of gluten/GG-1.5% on the skin and after peel-off. This observation implied that gluten/GG-1.5% could be a good biocompatible strain sensor [52, 53]. However, the test of biocompatibility with

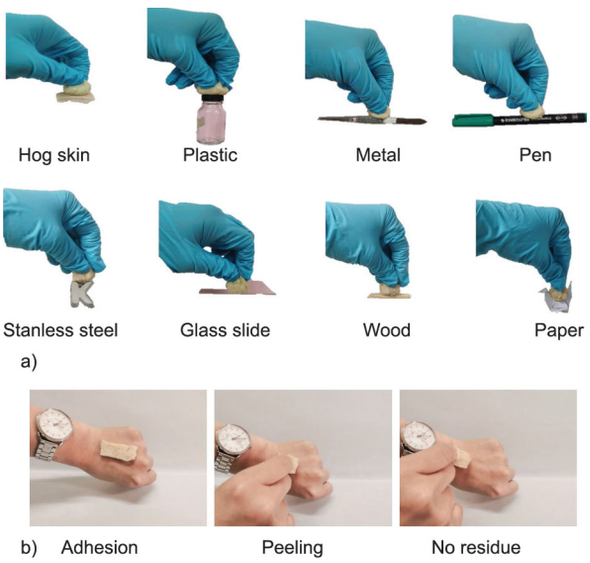

Figure 5. Adhesion of gluten/GG-1.5% smart strain sensor: (a) photographs of the gluten/GG-1.5% adhering to various types of substrates and (b) peeling test on human skin of gluten/GG-1.5%.

human cells and animals should be further studied to confirm the biocompatibility for a wide range of applications [54, 55].

The repeatability of the adhesion process through multiple adhesion-removal cycles was investigated, as illustrated in Figure 6a. The adhesive strength of gluten/GG-1.5% on three substrates decreased when the number of cycles increased. After 10 cycles, the adhesive strength of the gluten/GG-1.5% to wood, paper, and glass was 5.56, 4.31, and 1.22 kPa, respectively. The decrease in adhesive strength might be due to failure or contamination of the sample after repeated bonding [30]. The bonding efficiency of the gluten/GG-1.5% after 10 cycles was 58.56% for wood, 50.52% for paper, and 81.90% for glass, as shown in Figure 6b. Among three substrates, the adhesive strength on paper remarkably decreased. This was presumably because the entrapped polymer in the paper surface wrinkles during each cycle of the lap shear test resulted in a reduction of the contact area between adhesive and paper substrate [55]. The paper surface had the most wrinkles, as shown in Figure 7. The decrease in the bonding efficiency of gluten/GG-1.5% after 10 test cycles was in an acceptable range. In comparison, the bonding efficiency of an acrylated dopamine/gelatin hydrogel decreased to 60% after 5 cycles [30]. The long-term stability of the self-adhesive property was also observed, as shown in Figure 6c. The adhesive strength of gluten/GG-1.5% for three substrates decreased when the storage time increased. Sartori *et al*. [32] observed that during storage, the gluten adhesive containing glycerol could change its conformational structure, and the glycerol molecules slowly migrated from inside the matrix to the surface, resulting in a decrease in adhesive strength.

3.3. Conductivity of gluten/GG-1.5wt% strain sensor

The conductivity and stretchability of strain sensors are important properties for movement detection [56]. The gluten/GG-1.5% had conductivity of 0.12 S/m and stretchability of 465%, as shown in Table 1. The crosslinking of borax in the network of gluten, GG and glycerol created borate ions that acted as polyelectrolyte [17, 56]. The gauge factor (*GF*) of gluten/GG-1.5% was also determined to represent the responsiveness of the sensor to external stimuli. The *GF* can be calculated from the plot of resistance change ratio variation ($\Delta R/R_0$) versus strain. The resistance response as function of strain is shown in Figure 8. Under tensile deformation, free boronate ions were allowed to disperse and rearrange in the polymer network which led to a decrease in the ion concentration per unit volume and change in resistance [57]. The *GF* values of gluten/GG-1.5% at various strain ranges of 0-100, 100-280, 280-400 and 400-465 were 0.57, 0.15, 0.26, and 0.14, respectively. The obtained strain sensor based on gluten/GG-1.5% had *GF*, conductivity and stretchability comparable to those in the previous reports, as summarized in Table 1.

3.4. Long-term stability of gluten/GG-1.5% for smart functions and applications

Long-term stability is an important characteristic for actual application [56]. The water retention ability is a critical parameter that indicates the long-term stability of hydrogel-based sensors. Figure 9a shows that the water retention ability of gluten/GG-1.5% at 25 °C and 62% RH was 99.42–99.93% over 7 days of storage. The water retention capacity only slightly decreased with increasing storage time. The presence of glycerol in the sample can capture the water molecules via the interaction of hydroxyl groups which can lower the freezing point of water and decrease water evaporation [62]. This observation was confirmed by the DSC thermogram shown in Figure 9b. The exothermic peak due to water crystallization was clearly observed for gluten/GG-1.5% without glycerol, while a small exothermic peak was observed

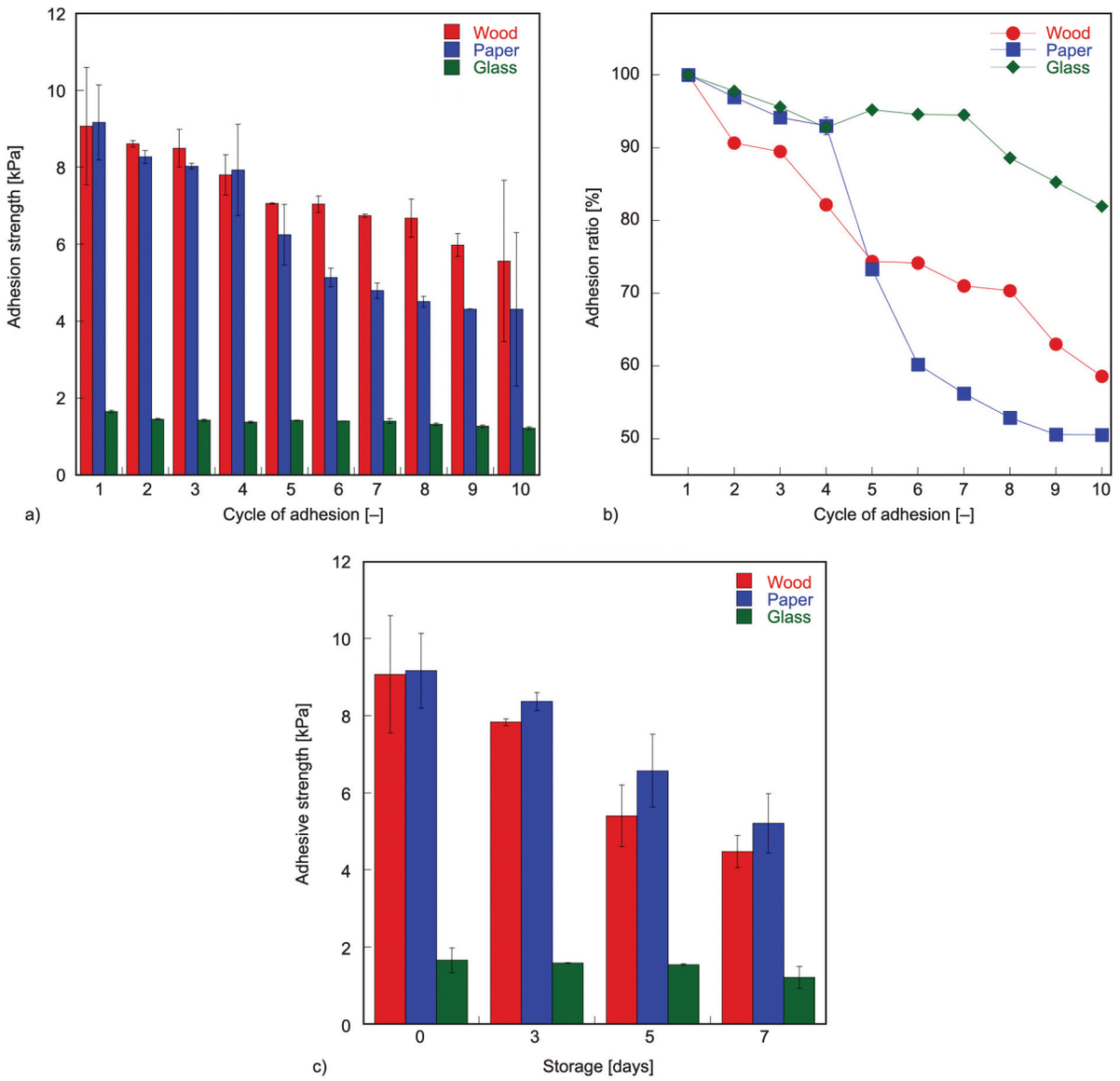

Figure 6. Adhesion of gluten/GG-1.5% smart strain sensor: (a) adhesion strength, (b) adhesion ratio of 10 times cyclic peeling tests on the three substrates, (c) long-term stability of self-adhesive property after storage times of 0, 3, 5, and 7 days.

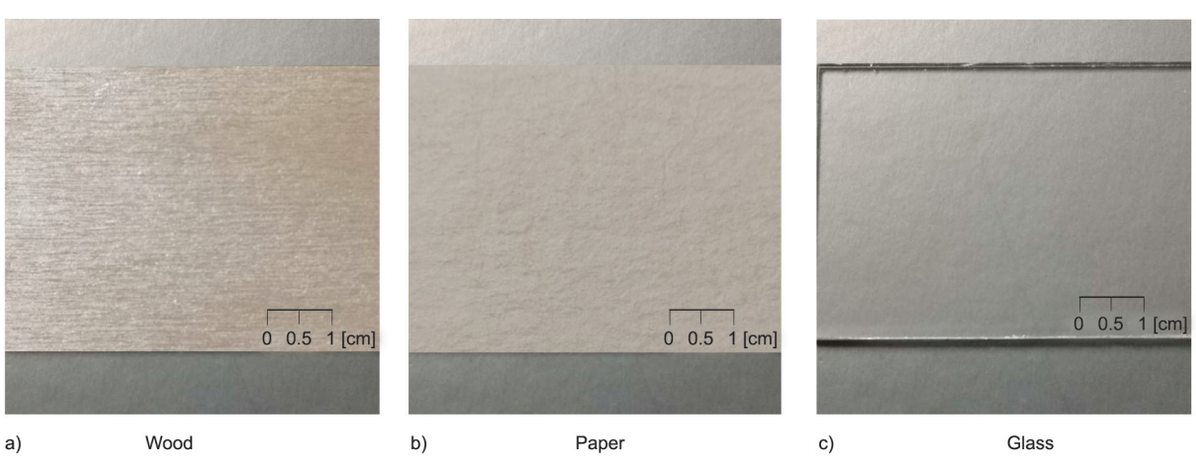

Figure 7. Surfaces of wood (a), paper (b) and glass (c).

Table 1. Comparison of strain sensors properties.

Strain sensor	Conductivity [S/m]	*GF* [–]	Stretchability [%]	Reference
Electrospun polyurethane microfiber	10.00	0.30–1.40	50	[58]
Single wall carbon nanotube hydrogel	–	0.24–1.51	100–1000	[59]
Dopamine–talc polyacrylamide hydrogel	–	0.13–0.63	100–1000	[60]
Poly(vinyl alcohol) /poly(vinylpyrrolidone) hydrogel	–	0.48	0–200	[61]
Gluten/GG-1.5%	0.12	0.14–0.57	0–465	Present study

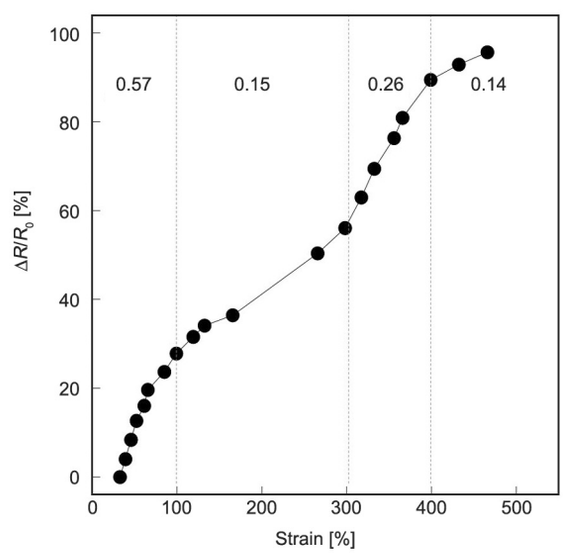

Figure 8. Relative change in resistance during stretching of gluten/GG-1.5%.

for gluten/GG-1.5%. This indicated a binding interaction between hydroxyl groups of glycerol and water molecules which rendered the growth of ice crystals [63].

Figure 10 and Figure 11 demonstrate the smart functions such as self-healing and remolding over the storage time of gluten/GG-1.5%, respectively. The self-healing and remolding behaviors of gluten/GG-1.5% resulted from dynamic and reversible multi-complexation among the hydroxyl groups of gluten, GG, water, glycerol, and borax. The soluble borax in water can promote borate ions and boric acid to create the crosslink with hydroxyl groups of gluten and GG. A similar reaction also occurs for glycerol and water. The hydroxyl groups of glycerol chelate with borax and combine with water to form a network of borax-glycerol-water [17, 56]. Figure 10 shows the self-healing process of gluten/GG-1.5%. The sample was cut into two pieces, and one piece of the sample was dyed red. The two pieces were kept in contact at room temperature, and after 3 h, the self-healing ability was tested by lifting a weight of 10 g. The gluten/GG-1.5% stored for 0–7 days could withstand the weight without any damage. This observation indicated a good self-healing efficiency and long-term stability. The main focus of this study was on the self-healing ability as a function of storage time, and in order to consolidate the self-healing time and reversible ability of ionic coordination in the hydrogel network [55], the rheological properties should be

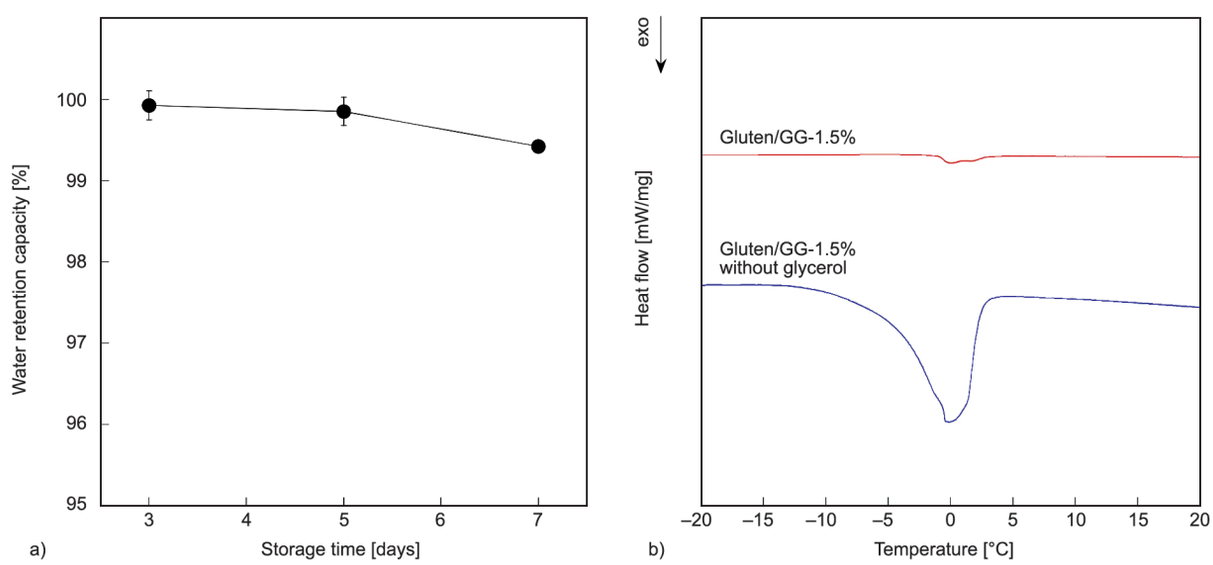

Figure 9. (a) water retention capacity of gluten/GG-1.5% and (b) DSC thermogram of gluten/GG-1.5%.

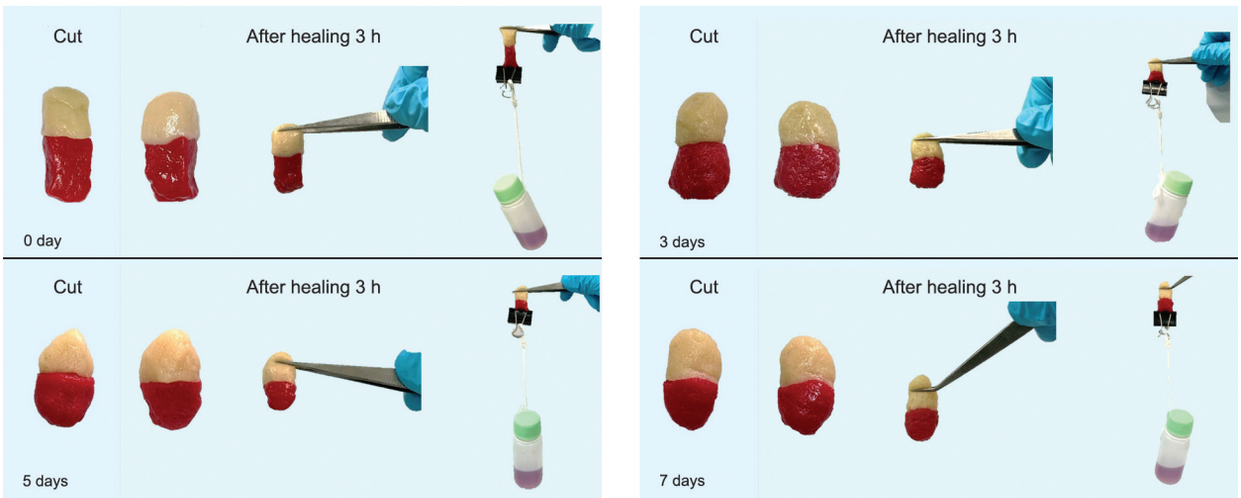

Figure 10. Self-healing properties of gluten/GG-1.5% over storage time.

further investigated. The remolding capability of gluten/GG-1.5% is shown in Figure 11. The gluten/GG-1.5% could be remolded into various shapes. The reshaped sample could also be connected with an electrical circuit to illuminate a LED indicator. After storage of gluten/GG-1.5% for 0, 3, 5, and

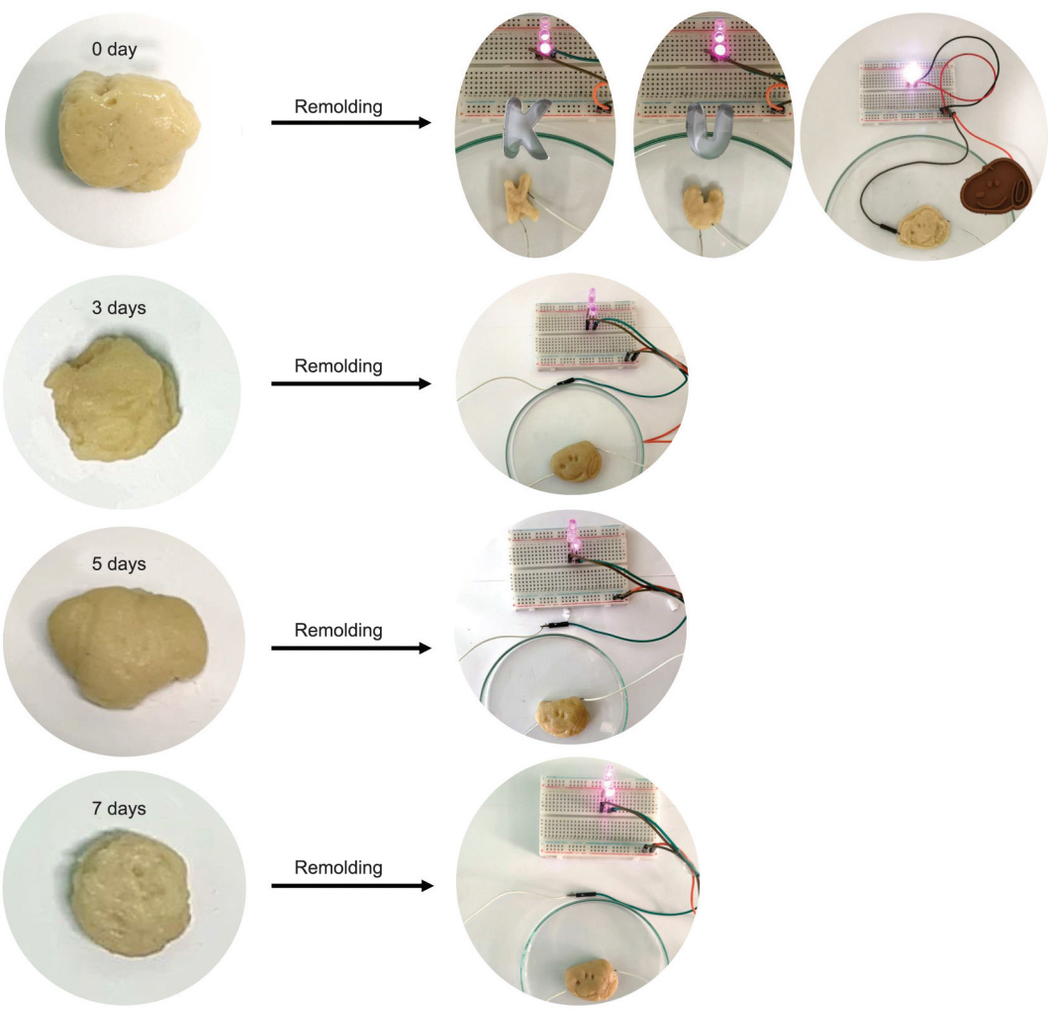

Figure 11. Remolding properties of gluten/GG-1.5% over storage time and circuit containing remolded gluten/GG-1.5% connected in a series with the LED.

7 days, the sample could be perfectly remolded. The connected LED circuit with gluten/GG-1.5% showed a constant brightness.

Application of gluten/GG-1.5% as a strain sensor and a self-powered device to detect human limb movements was studied. The gluten/GG-1.5% could detect the movement of a finger, a wrist, and a knee, as depicted in Figure 12. At the relaxation state, the sensor generated the minimum current. This current signal increased and reached the highest value when the sensor was bent [64]. The long-term stability of the strain sensor can be evaluated by the reproducibility and the stability of the signals of repeated movements over a period of storage [65]. After storage of gluten/GG-1.5% for 3 days, it was found that the gluten/GG-1.5% could detect the movement of a wrist, giving signals which were consistent and reproducible, as shown in Figure 13. After 5 days of storage, unstable signals from movements were observed. The gluten/GG-1.5% did not perfectly adhere to the wrist after 5 days due to glycerol migration. This observation corresponded to the decrease in adhesive strength, as depicted in Figure 6c. A decrease in the contact area between the strain sensor and epidermal surface resulted in a low response for relative resistance [66]. Furthermore, dehydration of the hydrogel during storage was another factor that affected the loss of electrical conductivity, flexibility, and sensing ability [67].

Figure 14 shows the self-powered ability of gluten/GG-1.5%. The gluten/GG-1.5% was placed between a zinc sheet and a copper sheet and then connected with wires to form a circuit, as shown in Figure 15. The presence of gluten/GG-1.5% as an electrolyte allowed

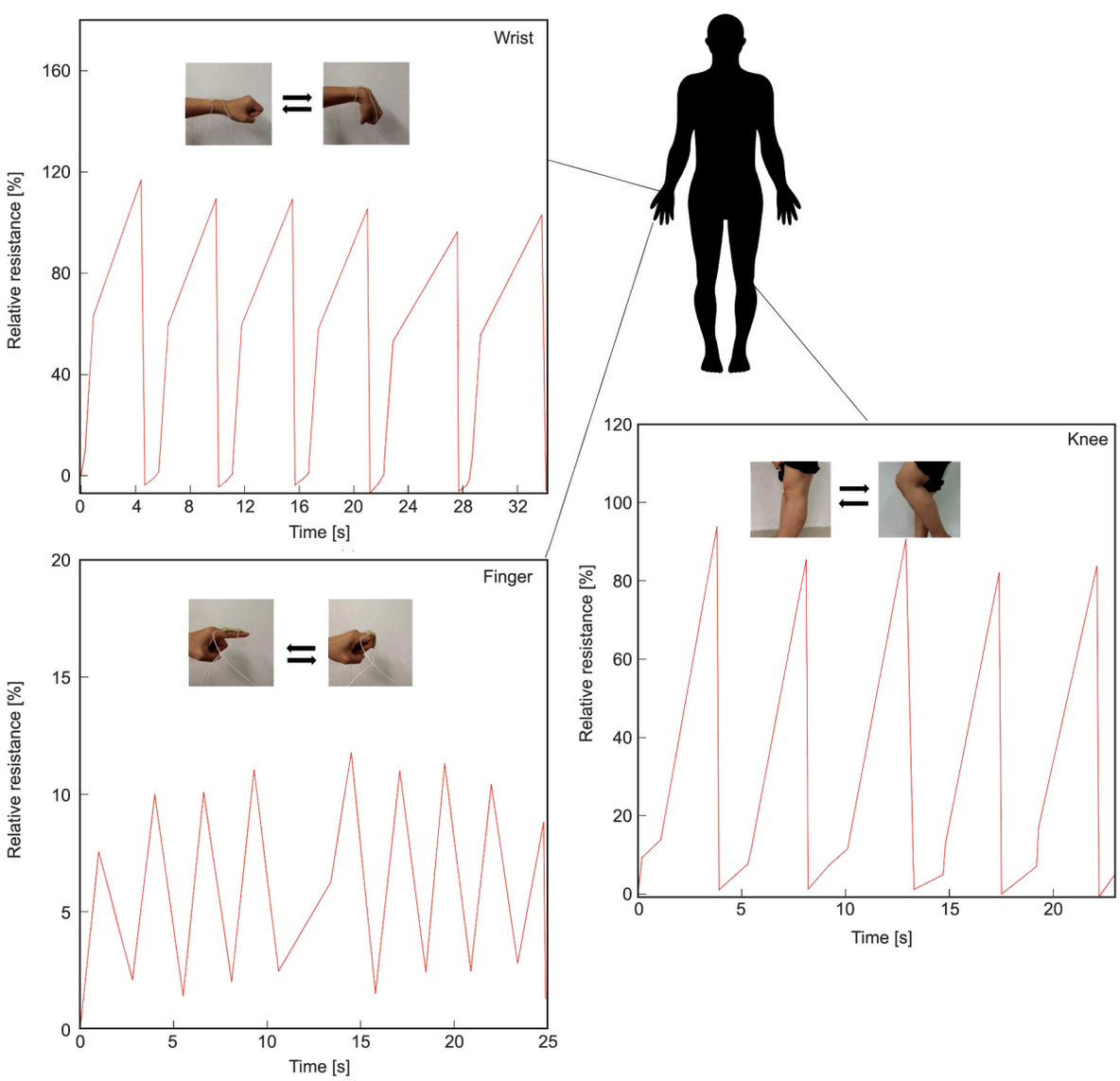

Figure 12. Demonstration of gluten/GG-1.5% smart strain sensor of monitoring physical motions.

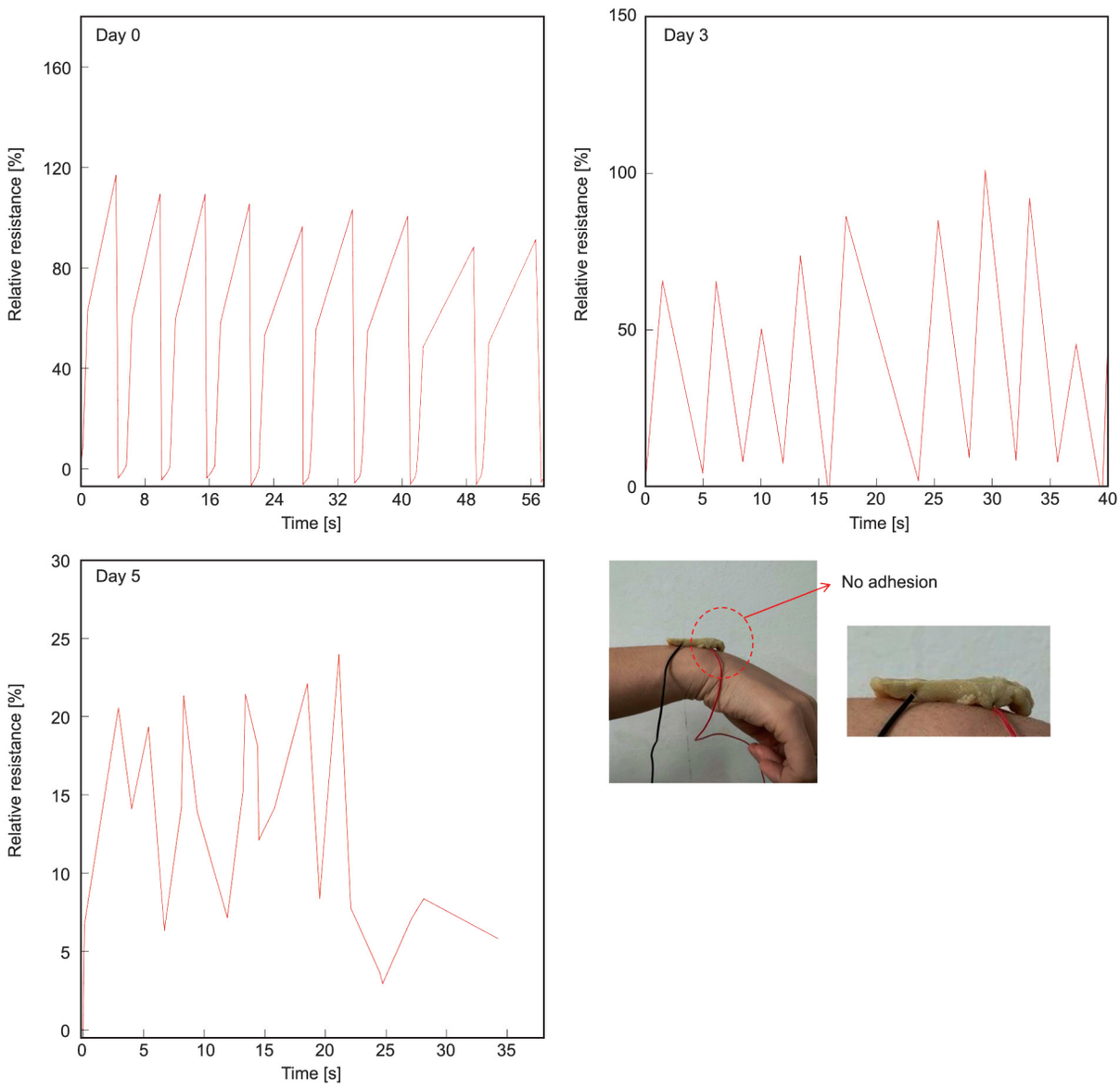

Figure 13. The gluten/GG-1.5% smart strain sensor of wrist monitoring motions under storage time.

redox reactions between the two metal electrodes (zinc and copper sheets) to occur. The self-powered gluten/GG-1.5% showed a stable response to compression. A current increased during compression and reduced when the sample recovered to its original state. This is because the ionic conductivity of the electrolyte is determined by ion mobility, which can also be altered by the distance between the two electrodes and the contact between the electrode and electrolyte interface. During compression, the distance between the two metal sheets is lowered, and possibly improved adhesion between the electrodes and electrolyte is achieved, thereby increasing the ionic conductivity and lowering the resistance. The resistance increases again as the sample recovered to its original state because of the larger distance between the electrodes and lower adhesion between the electrodes and electrolyte. The self-powered gluten/GG-1.5% showed good sensitivity and stability over 7 days of the experiment, with currents in the range of 0.05–14.4 μA. The obtained currents after 7 days storage were comparable to those of self-powered hydrogels in the previous reports such as polyethylene terephthalate/zinc oxide nanowires (2.5 μA) [64], ionic organohydrogel (7.5–16 μA) [24], and polydimethylsiloxane/tin sulfide (30–60 nA) [68].

4. Conclusions

In conclusion, a multifunctional smart strain sensor based on gluten/GG copolymer was successfully developed. The gluten/GG strain sensor with combined

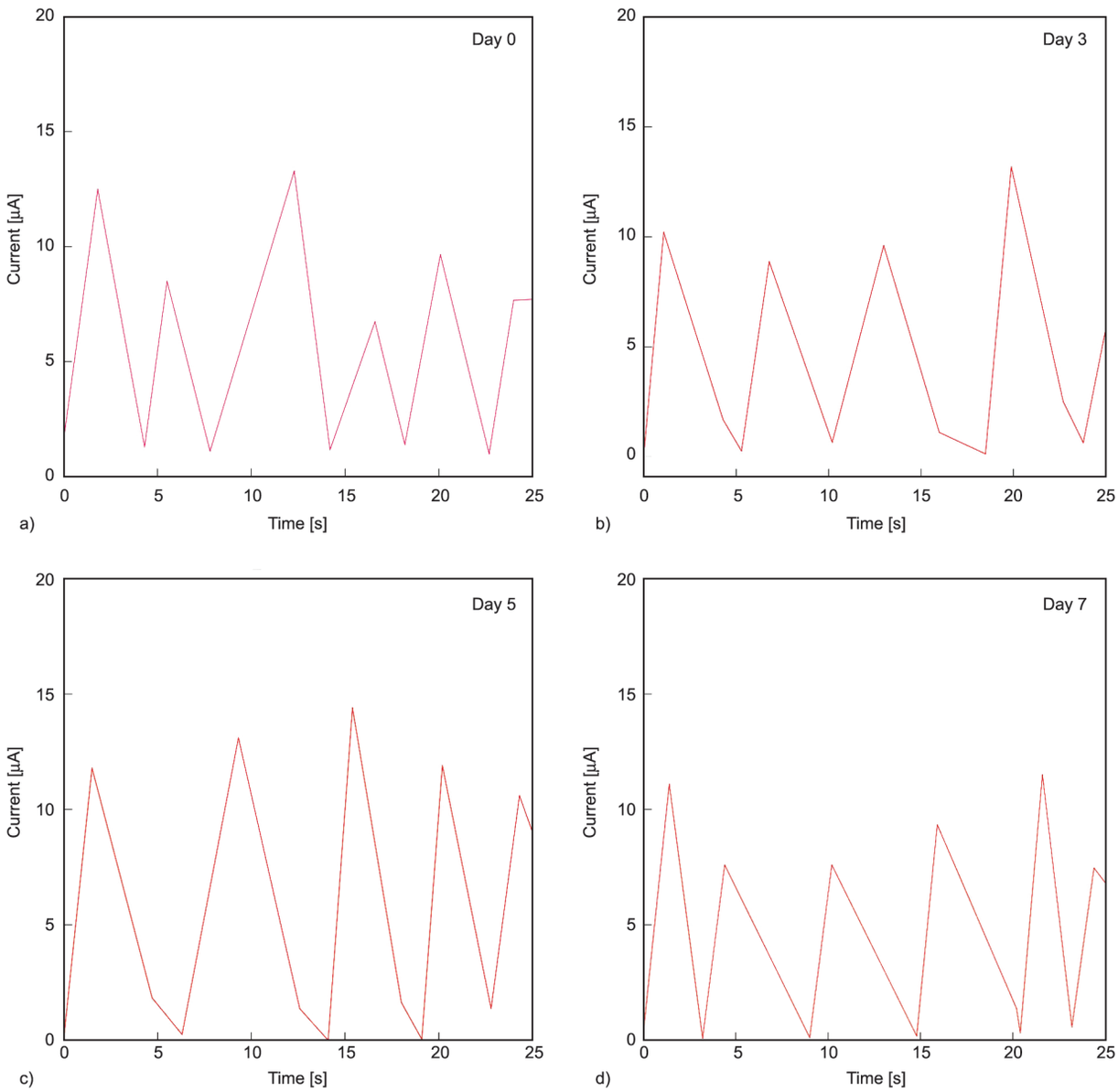

Figure 14. Electrical signal response curves of gluten/GG-1.5% smart strain sensor at storage times of 0 (a), 3 (b), 5 (c), and 7 days (d).

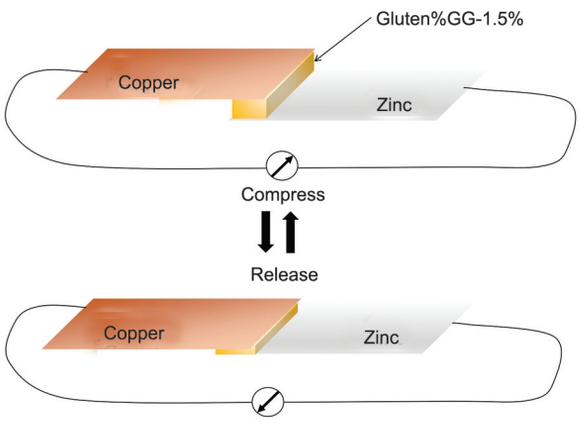

Figure 15. Schematic representation of gluten/GG-1.5% smart strain sensor-based self-powered pressure sensor.

multifunctional capabilities such as self-healing, remolding, and self-powering ability provided long-term stability over 7 days. The gluten/GG-1.5% proved to be the most suitable blend showing the greatest adhesive strength on various substrates. Moreover, the gluten/GG-1.5% also demonstrated reproducibility up to 10 cycles with an acceptable loss of adhesive strength. The gluten/GG-1.5% stored for 3 days could detect wrist movement with good reproducibility and stability. All these features make the multifunctional strain sensor based on gluten/GG-1.5% a highly desirable material for smart engineering devices.

Acknowledgements

This work was supported by Research and Graduate Studies Khon Kaen University. The authors would also like to thank the Royal Golden Jubilee Ph.D. scholarship of the Thailand Research Fund [grant number PHD/0220/2560].

References

[1] Lv Z., Liu J., Yang X., Fan D., Cao J., Luo Y., Zhang X.: Naturally derived wearable strain sensors with enhanced mechanical properties and high sensitivity. ACS Applied Materials and Interfaces, **12**, 22163–22169 (2020). https://doi.org/10.1021/acsami.0c04341

[2] Nakaramontri Y., Kummerlöwe C., Nakason C., Pichaiyut S., Wisunthon S., Clemens F.: Piezoresistive carbon-based composites for sensor applications: Effects of polarity and non-rubber components on shape recovery. Express Polymer Letters, **14**, 970–986 (2020). https://doi.org/10.3144/expresspolymlett.2020.79

[3] Song Y. X., Xu W. M., Rong M. Z., Zhang M. Q.: A sunlight self-healable fibrous flexible pressure sensor based on electrically conductive composite wool yarns. Express Polymer Letters, **14**, 1089–1104 (2020). https://doi.org/10.3144/expresspolymlett.2020.88

[4] Tang N., Zhou C., Qu D., Fang Y., Zheng Y., Hu W., Jin K., Wu W., Duan X., Haick H.: A highly aligned nanowire-based strain sensor for ultrasensitive monitoring of subtle human motion. Small, **16**, 2001363 (2020). https://doi.org/10.1002/smll.202001363

[5] Wang S., Fang Y., He H., Zhang L., Li C., Ouyang J.: Wearable stretchable dry and self-adhesive strain sensors with conformal contact to skin for high-quality motion monitoring. Advanced Functional Materials, **31**, 2007495 (2021). https://doi.org/10.1002/adfm.202007495

[6] Yang C., Yin J., Chen Z., Du H., Tian M., Zhang M., Zheng J., Ding L., Zhang P., Zhang X., Deng K.: Highly conductive, stretchable, adhesive, and self-healing polymer hydrogels for strain and pressure sensor. Macromolecular Materials and Engineering, **305**, 2000479 (2020). https://doi.org/10.1002/mame.202000479

[7] Qin H., Chen Y., Huang J., Wei Q.: Bacterial cellulose reinforced polyaniline electroconductive hydrogel with multiple weak H-bonds as flexible and sensitive strain sensor. Macromolecular Materials and Engineering, **306**, 2100159 (2021). https://doi.org/10.1002/mame.202100159

[8] Asha A. B., Chen Y., Zhang H., Ghaemi S., Ishihara K., Liu Y., Narain R.: Rapid mussel-inspired surface zwitteration for enhanced antifouling and antibacterial properties. Langmuir, **35**, 1621–1630 (2019). https://doi.org/10.1021/acs.langmuir.8b03810

[9] Ghahri S., Bari E., Pizzi A. A.: The challenge of environment-friendly adhesives for bio-composites. in 'Eco-friendly adhesives for wood and natural fiber composites' (eds.: Jawaid M., Khan T. A., Nasir M., Asim M.) Springer, Singapore 1975–229 (2021). https://doi.org/10.1007/978-981-33-4749-6_11

[10] Han X., Lu W., Yu W., Xu H., Bi S., Cai H.: Conductive and adhesive gluten ionic skin for eco-friendly strain sensor. Journal of Materials Science, **56**, 3970–3980 (2021). https://doi.org/10.1007/s10853-020-05508-3

[11] Han S., Liu C., Lin X., Zheng J., Wu J., Liu C.: Dual conductive network hydrogel for a highly conductive, self-healing, anti-freezing, and non-drying strain sensor. ACS Applied Polymer Materials, **2**, 996–1005 (2020). https://doi.org/10.1021/acsapm.9b01198

[12] Cheng B., Chang S., Li H., Li Y., Shen W., Shang Y., Cao A.: Highly stretchable and compressible carbon nanofiber–polymer hydrogel strain sensor for human motion detection. Macromolecular Materials and Engineering, **305**, 1900813 (2020). https://doi.org/10.1002/mame.201900813

[13] Chen W., Bu Y., Li D., Liu Y., Chen G., Wan X., Li N.: Development of high-strength, tough, and self-healing carboxymethyl guar gum-based hydrogels for human motion detection. Journal of Materials Chemistry C, **8**, 900–908 (2020). https://doi.org/10.1039/C9TC05797H

[14] Sharma S., Afgan S., Deepak, Kumar A., Kumar R.: L-alanine induced thermally stable self-healing guar gum hydrogel as potential drug vehicle for sustained release of hydrophilic drug. Materials Science and Engineering: C, **99**, 1384–1391 (2019). https://doi.org/10.1016/j.msec.2019.02.074

[15] Sun Z., Wang L., Jiang X., Bai L., Wang W., Chen H., Yang L., Yang H., Wei D.: Self-healing, sensitive and antifreezing biomass nanocomposite hydrogels based on hydroxypropyl guar gum and application in flexible sensors. International Journal of Biological Macromolecules, **155**, 1569–1577 (2020). https://doi.org/10.1016/j.ijbiomac.2019.11.134

[16] Baudouin F., Nogueira T. L., van der Mijnsbrugge A., Frederix S., Redl A., Morel M. H.: Mechanochemical activation of gluten network development during dough mixing. Journal of Food Engineering, **283**, 110035 (2020). https://doi.org/10.1016/j.jfoodeng.2020.110035

[17] Pan X., Wang Q., Ning D., Dai L., Liu K., Ni Y., Chen L., Huang L.: Ultraflexible self-healing guar gum-glycerol hydrogel with injectable, antifreeze, and strain-sensitive properties. ACS Biomaterials Science and Engineering, **4**, 3397–3404 (2018). https://doi.org/10.1021/acsbiomaterials.8b00657

[18] Liu S., Wang X., Peng Y., Wang Z., Ran R.: Highly stretchable, strain-sensitive, and antifreezing macromolecular microsphere composite starch-based hydrogel. Macromolecular Materials and Engineering, **306**, 2100198 (2021).
https://doi.org/10.1002/mame.202100198

[19] Liu C., McClements D. J., Li M., Xiong L., Sun Q.: Development of self-healing double-network hydrogels: Enhancement of the strength of wheat gluten hydrogels by *in situ* metal–catechol coordination. Journal of Agricultural and Food Chemistry, **67**, 6508–6516 (2019).
https://doi.org/10.1021/acs.jafc.9b01649

[20] Zhu J., Guan S., Hu Q., Gao G., Xu K., Wang P.: Tough and pH-sensitive hydroxypropyl guar gum/polyacrylamide hybrid double-network hydrogel. Chemical Engineering Journal, **306**, 953–960 (2016).
https://doi.org/10.1016/j.cej.2016.08.026

[21] Gong J. P., Katsuyama Y., Kurokawa T., Osada Y.: Double-network hydrogels with extremely high mechanical strength. Advanced Materials, **15**, 1155–1158 (2003).
https://doi.org/10.1002/adma.200304907

[22] Li G., Zhang H., Fortin D., Xia H., Zhao Y.: Poly(vinyl alcohol)–poly(ethylene glycol) double-network hydrogel: A general approach to shape memory and self-healing functionalities. Langmuir, **31**, 11709–11716 (2015).
https://doi.org/10.1021/acs.langmuir.5b03474

[23] Rao Z., Liu S., Wu R., Wang G., Sun Z., Bai L., Wang W., Chen H., Yang H., Wei D., Niu Y.: Fabrication of dual network self-healing alginate/guar gum hydrogels based on polydopamine-type microcapsules from mesoporous silica nanoparticles. International Journal of Biological Macromolecules, **129**, 916–926 (2019).
https://doi.org/10.1016/j.ijbiomac.2019.02.089

[24] Huang J., Peng S., Gu J., Chen G., Gao J., Zhang J., Hou L., Yang X., Jiang X., Guan L.: Self-powered integrated system of a strain sensor and flexible all-solid-state supercapacitor by using a high performance ionic organohydrogel. Materials Horizons, **7**, 2085–2096 (2020).
https://doi.org/10.1039/D0MH00100G

[25] Wang J., Tang F., Wang Y., Lu Q., Liu S., Li L.: Self-healing and highly stretchable gelatin hydrogel for self-powered strain sensor. ACS Applied Materials and Interfaces, **12**, 1558–1566 (2019).
https://doi.org/10.1021/acsami.9b18646

[26] Chen C. Y., Tsai C. Y., Xu M. H., Wu C. T., Huang C. Y., Lee T. H., Fuh Y. K.: A fully encapsulated piezoelectric-triboelectric hybrid nanogenerator for energy harvesting from biomechanical and environmental sources. Express Polymer Letters, **13**, 533–542 (2019).
https://doi.org/10.3144/expresspolymlett.2019.45

[27] Kim J. N., Lee J., Lee H., Oh I. K.: Stretchable and self-healable catechol-chitosan-diatom hydrogel for triboelectric generator and self-powered tremor sensor targeting at Parkinson disease. Nano Energy, **82**, 105705 (2021).
https://doi.org/10.1016/j.nanoen.2020.105705

[28] Jing X., Feng P., Chen Z., Xie Z., Li H., Peng X-F., Mi H-Y., Liu Y.: Highly stretchable, self-healable, freezing-tolerant, and transparent polyacrylic acid/nanochitin composite hydrogel for self-powered multifunctional sensors. ACS Sustainable Chemistry and Engineering, **9**, 9209–9220 (2021).
https://doi.org/10.1021/acssuschemeng.1c00949

[29] Ma C., Pang H., Liu H., Yan Q., Li J., Zhang S.: A tough, adhesive, self-healable, and antibacterial plant-inspired hydrogel based on pyrogallol-borax dynamic cross-linking. Journal of Materials Chemistry B, **9**, 4230–4240 (2021).
https://doi.org/10.1039/D1TB00763G

[30] Zhou Z., He Z., Yin S., Xie X., Yuan W.: Adhesive, stretchable and antibacterial hydrogel with external/self-power for flexible sensitive sensor used as human motion detection. Composites Part B: Engineering, **220**, 108984 (2021).
https://doi.org/10.1016/j.compositesb.2021.108984

[31] Min S-H., Lee G-Y., Ahn S-H.: Direct printing of highly sensitive, stretchable, and durable strain sensor based on silver nanoparticles/multi-walled carbon nanotubes composites. Composites Part B: Engineering, **161**, 395–401 (2019).
https://doi.org/10.1016/j.compositesb.2018.12.107

[32] Sartori T., Feltre G., do Amaral Sobral P. J., da Cunha R. L., Menegalli F. C.: Biodegradable pressure sensitive adhesives produced from vital wheat gluten: Effect of glycerol as plasticizer. Colloids and Surfaces A: Physicochemical and Engineering Aspects, **560**, 42–49 (2019).
https://doi.org/10.1016/j.colsurfa.2018.09.069

[33] Hazrol M. D., Sapuan S. M., Zainudin E. S., Zuhri M. Y. M., Abdul Wahab N. I.: Corn starch (*Zea mays*) biopolymer plastic reaction in combination with sorbitol and glycerol. Polymers, **13**, 242 (2021).
https://doi.org/10.3390/polym13020242

[34] Sarkar D. J., Singh A.: pH-triggered release of boron and thiamethoxam from boric acid crosslinked carboxymethyl cellulose hydrogel based formulations. Polymer-Plastics Technology and Materials, **58**, 83–96 (2019).
https://doi.org/10.1080/03602559.2018.1466165

[35] Bagheri A., Nazari A., Hajimohammadi A., Sanjayan J. G., Rajeev P., Nikzad M., Ngo T., Mendis P.: Microstructural study of environmentally friendly boroaluminosilicate geopolymers. Journal of Cleaner Production, **189**, 805–812 (2018).
https://doi.org/10.1016/j.jclepro.2018.04.034

[36] Dasineh S., Akbarian M., Ebrahimi H. A., Behbudi G.: Tacrolimus-loaded chitosan-coated nanostructured lipid carriers: Preparation, optimization and physicochemical characterization. Applied Nanoscience, **11**, 1169–1181 (2021).
https://doi.org/10.1007/s13204-021-01744-4

[37] Dateraksa K., Sinchai S.: Phase formation of boron carbide powder synthesized from glutinous rice flour. Journal of Metals, Materials and Minerals, **29**, 48–53 (2019).
https://doi.org/10.14456/jmmm.2019.33

[38] Ma C., Pang H., Liu H., Yan Q., Li J., Zhang S.: A tough, adhesive, self-healable, and antibacterial plant-inspired hydrogel based on pyrogallol-borax dynamic cross-linking. Journal of Materials Chemistry B, **9**, 4230–4240 (2021). https://doi.org/10.1039/d1tb00763g

[39] Fu Q., Chen Y., Sorieul M.: Wood-based flexible electronics. ACS Nano, **14**, 3528–3538 (2020). https://doi.org/10.1021/acsnano.9b09817

[40] Liu H., Jiang H., Du F., Zhang D., Li Z., Zhou H.: Flexible and degradable paper-based strain sensor with low cost. ACS Sustainable Chemistry and Engineering, **5**, 10538–10543 (2017). https://doi.org/10.1021/acssuschemeng.7b02540

[41] Liu L., Jiao Z., Zhang J., Wang Y., Zhang C., Meng X., Jiang X., Niu S., Han Z., Ren L.: Bioinspired, superhydrophobic, and paper-based strain sensors for wearable and underwater applications. ACS Applied Materials and Interfaces, **13**, 1967–1978 (2021). https://doi.org/10.1021/acsami.0c18818

[42] Xia S., Song S., Jia F., Gao G.: A flexible, adhesive and self-healable hydrogel-based wearable strain sensor for human motion and physiological signal monitoring. Journal of Materials Chemistry B, **7**, 4638–4648 (2019). https://doi.org/10.1039/c9tb01039d

[43] Zhao L., Ke T., Ling Q., Liu J., Li Z., Gu H.: Multifunctional ionic conductive double-network hydrogel as a long-term flexible strain sensor. ACS Applied Polymer Materials, **3**, 5494–5508 (2021). https://doi.org/10.1021/acsapm.1c00805

[44] Liao M., Wan P., Wen J., Gong M., Wu X., Wang Y., Shi R., Zhang L.: Wearable, healable, and adhesive epidermal sensors assembled from mussel-inspired conductive hybrid hydrogel framework. Advanced Functional Materials, **27**, 1703852 (2017). https://doi.org/10.1002/adfm.201703852

[45] Norström E., Fogelström L., Nordqvist P., Khabbaz F., Malmström E.: Gum dispersions as environmentally friendly wood adhesives. Industrial Crops and Products, **52**, 736–744 (2014). https://doi.org/10.1016/j.indcrop.2013.12.001

[46] Xi S., Tian F., Wei G., He X., Shang Y., Ju Y., Li W., Lu Q., Wang Q.: Reversible dendritic-crystal-reinforced polymer gel for bioinspired adaptable adhesive. Advanced Materials, **33**, 2103174 (2021). https://doi.org/10.1002/adma.202103174

[47] Bradley L. C., Bade N. D., Mariani L. M., Turner K. T., Lee D., Stebe K. J.: Rough adhesive hydrogels (RAd gels) for underwater adhesion. ACS Applied Materials and Interfaces, **9**, 27409–27413 (2017). https://doi.org/10.1021/acsami.7b08916

[48] Severijns C., de Freitas S. T., Poulis J. A.: Susceptor-assisted induction curing behaviour of a two component epoxy paste adhesive for aerospace applications. International Journal of Adhesion and Adhesives, **75**, 155–164 (2017). https://doi.org/10.1016/j.ijadhadh.2017.03.005

[49] Wang T., Ren X., Bai Y., Liu L., Wu G.: Adhesive and tough hydrogels promoted by quaternary chitosan for strain sensor. Carbohydrate Polymers, **254**, 117298 (2021). https://doi.org/10.1016/j.carbpol.2020.117298

[50] Wei X., Ma K., Cheng Y., Sun L., Chen D., Zhao X., Lu H., Song B., Yang K., Jia P.: Adhesive, conductive, self-healing, and antibacterial hydrogel based on chitosan–polyoxometalate complexes for wearable strain sensor. ACS Applied Polymer Materials, **2**, 2541–2549 (2020). https://doi.org/10.1021/acsapm.0c00150

[51] Chen H., Xu Z., Mo J., Lyu Y., Tang X., Shen X.: Effects of guar gum on adhesion properties of soybean protein isolate onto porcine bones. International Journal of Adhesion and Adhesives, **75**, 124–131 (2017). https://doi.org/10.1016/j.ijadhadh.2017.03.001

[52] An R., Zhang B., Han L., Wang X., Zhang Y., Shi L., Ran R.: Strain-sensitivity conductive MWCNTs composite hydrogel for wearable device and near-infrared photosensor. Journal of Materials Science, **54**, 8515–8530 (2019). https://doi.org/10.1007/s10853-019-03438-3

[53] Sun H., Zhou K., Yu Y., Yue X., Dai K., Zheng G., Liu C., Shen C.: Highly stretchable, transparent, and biofriendly strain sensor based on self-recovery ionic-covalent hydrogels for human motion monitoring. Macromolecular Materials and Engineering, **304**, 1900227 (2019). https://doi.org/10.1002/mame.201900227

[54] Zheng B-D., Ye J., Yang Y-C., Huang Y-Y., Xiao M-T.: Self-healing polysaccharide-based injectable hydrogels with antibacterial activity for wound healing. Carbohydrate Polymers, **275**, 118770 (2022). https://doi.org/10.1016/j.carbpol.2021.118770

[55] Wang H., Xu Z., Zhao M., Liu G., Wu J.: Advances of hydrogel dressings in diabetic wounds. Biomaterials Science, **9**, 1530–1546 (2021). https://doi.org/10.1039/d0bm01747g

[56] Taesuwan I., Ounkaew A., Okhawilai M., Hiziroglu S., Jarernboon W., Chindaprasirt P., Kasemsiri P.: Smart conductive nanocomposite hydrogel containing green synthesized nanosilver for use in an eco-friendly strain sensor. Cellulose, **29**, 273–286 (2021). https://doi.org/10.1007/s10570-021-04302-x

[57] Wang Y., Huang H., Wu J., Han L., Yang Z., Jiang Z., Wang R., Huang Z., Xu M.: Ultrafast self-healing, reusable, and conductive polysaccharide-based hydrogels for sensitive ionic sensors. ACS Sustainable Chemistry and Engineering, **8**, 18506–18518 (2020). https://doi.org/10.1021/acssuschemeng.0c06258

[58] Jeon H., Hong S. K., Cho S. J., Lim G.: Fabrication of a highly sensitive stretchable strain sensor utilizing a microfibrous membrane and a cracking structure on conducting polymer. Macromolecular Materials and Engineering, **303**, 1700389 (2018). https://doi.org/10.1002/mame.201700389

[59] Cai G., Wang J., Qian K., Chen J., Li S., Lee P. S.: Extremely stretchable strain sensors based on conductive self-healing dynamic cross-links hydrogels for human-motion detection. Advanced Science, **4**, 1600190 (2017). https://doi.org/10.1002/advs.201600190

[60] Jing X., Mi H. Y., Lin Y. J., Enriquez E., Peng X. F., Turng L. S.: Highly stretchable and biocompatible strain sensors based on mussel-inspired super-adhesive self-healing hydrogels for human motion monitoring. ACS Applied Materials and Interfaces, **10**, 20897–20909 (2018). https://doi.org/10.1021/acsami.8b06475

[61] Liu Y-J., Cao W-T., Ma M-G., Wan P.: Ultrasensitive wearable soft strain sensors of conductive, self-healing, and elastic hydrogels with synergistic 'soft and hard' hybrid networks. ACS Applied Materials and Interfaces, **9**, 25559–25570 (2017). https://doi.org/10.1021/acsami.7b07639

[62] Chen F., Zhou D., Wang J., Li T., Zhou X., Gan T., Handschuh-Wang S., Zhou X.: Rational fabrication of anti-freezing, non-drying tough organohydrogels by one-pot solvent displacement. Angewandte Chemie - International Edition, **57**, 6568–6571 (2018). https://doi.org/10.1002/anie.201803366

[63] Peng Y., Pi M., Zhang X., Yan B., Li Y., Shi L., Ran R.: High strength, antifreeze, and moisturizing conductive hydrogel for human-motion detection. Polymer, **196**, 122469 (2020). https://doi.org/10.1016/j.polymer.2020.122469

[64] Wang Q., Pan X., Zhang H., Cao S., Ma X., Huang L., Chen L., Ni Y.: Fruit-battery-inspired self-powered stretchable hydrogel-based ionic skin that works effectively in extreme environments. Journal of Materials Chemistry A, **9**, 3968–3975 (2021). https://doi.org/10.1039/D0TA09149A

[65] Yin J., Lu C., Li C., Yu Z., Shen C., Yang Y., Jiang X., Zhang Y.: A UV-filtering, environmentally stable, healable and recyclable ionic hydrogel towards multifunctional flexible strain sensor. Composites Part B: Engineering, **230**, 109528 (2022). https://doi.org/10.1016/j.compositesb.2021.109528

[66] Yin J., Pan S., Wu L., Tan L., Chen D., Huang S., Zhang Y., He P.: A self-adhesive wearable strain sensor based on a highly stretchable, tough, self-healing and ultrasensitive ionic hydrogel. Journal of Materials Chemistry C, **8**, 17349–17364 (2020). https://doi.org/10.1039/d0tc04144k

[67] Wu Z., Yang X., Wu J.: Conductive hydrogel- and organohydrogel-based stretchable sensors. ACS Applied Materials and Interfaces, **13**, 2128–2144 (2021). https://doi.org/10.1021/acsami.0c21841

[68] Yan W., Fuh H. R., Lv Y., Chen K. Q., Tsai T. Y., Wu Y. R., Shieh T. H., Hung K. M., Li J., Zhang D., Ó Coileáin C., Arora S. K., Wang Z., Jiang Z., Chang C. R., Wu H. C.: Giant gauge factor of van der Waals material based strain sensors. Nature Communications, **12**, 2018 (2021). https://doi.org/10.1038/s41467-021-22316-8